



HAL
open science

Dielectric behaviour of an epoxy network cured with a phosphonium-based ionic liquid

Thibaut Lefort, Jannick Duchet-Rumeau, Sébastien Livi, Damien Bachellerie, Sébastien Pruvost

► **To cite this version:**

Thibaut Lefort, Jannick Duchet-Rumeau, Sébastien Livi, Damien Bachellerie, Sébastien Pruvost. Dielectric behaviour of an epoxy network cured with a phosphonium-based ionic liquid. *Polymer*, 2021, 222, pp.123645. 10.1016/j.polymer.2021.123645 . hal-03279986

HAL Id: hal-03279986

<https://hal.science/hal-03279986>

Submitted on 24 Apr 2023

HAL is a multi-disciplinary open access archive for the deposit and dissemination of scientific research documents, whether they are published or not. The documents may come from teaching and research institutions in France or abroad, or from public or private research centers.

L'archive ouverte pluridisciplinaire **HAL**, est destinée au dépôt et à la diffusion de documents scientifiques de niveau recherche, publiés ou non, émanant des établissements d'enseignement et de recherche français ou étrangers, des laboratoires publics ou privés.



Distributed under a Creative Commons Attribution 4.0 International License

Dielectric behaviour of an epoxy network cured with a phosphonium-based ionic liquid

Thibaut Lefort^{1,2}, Jannick Duchet-Rumeau¹, Sébastien Livi¹, Damien Bachellerie² and Sébastien Pruvost^{1,*}

1 Univ. Lyon, INSA Lyon, UMR CNRS 5223, IMP Ingénierie des Matériaux Polymères, F-69621 Villeurbanne, France

2 SuperGrid Institute SAS- 23, rue Cyprian, BP 1321 - 69611 Villeurbanne, France

ABSTRACT

Phosphonium based ionic liquids (ILs) have been previously shown as a new emerging class of initiator of epoxy prepolymers. The present study aims at investigating the influence of ILs on the dielectric behaviour of epoxy-IL systems by dielectric spectroscopy. Here, the content of IL incorporated in the epoxy prepolymer has a significant impact on the final properties of the polymer networks displaying a high glass transition temperature ($T_g > 160$ °C). The excess of IL (> 10 phr) acts as a plasticizer agent decreasing the T_g and leading to the formation of heterogeneities. Moreover, the study of α and β conventional relaxation modes by dielectric spectroscopy highlighted an increase of chain mobility due to IL excess. A ω relaxation mode has been noticed with the addition of high content of IL, probably relating to heterogeneities of the network. Unlike the most of polymer systems, the study of the DC conductivity by the application of an Arrhenius law demonstrated a thermal activation mechanism, independent from the free volume and the glass transition phenomenon. A discussion on the identification of charge carriers has been finally proposed.

1 INTRODUCTION

Ionic liquids (ILs) are molten salts composed of an organic cation and an organic or inorganic anion with a melting temperature below 100°C. Due to their low vapour pressure, their good chemical and thermal stabilities, the endless number of cation-anion combinations, their high ionic conductivity and their ability as a solvent [1] [2]. ILs have recently attracted a great interest in the material science. Moreover, their low melting temperature as well as their tuneable viscosity allow them to be compatible with polymer process temperature. These properties make them attractive in a wide range of applications, such as electrolytes [3] [4] [5] [6] [7], lubricants [8] [9] [10], plasticizers and materials additives [11] [12].

Very recently, few authors investigated the ability of ILs to initiate the homopolymerization of epoxy prepolymers [13] [14] [15]. The first studies have reported that imidazolium and pyridinium based ILs were able through their decomposition products (the imidazolium is decomposed into an imidazole)

to open the epoxy ring of a prepolymer, and form an adduct including an alkoxide anion. Then the alkoxide propagates until the formation of a three-dimensional network by anionic polymerization [13].

Different mechanisms have been proposed for phosphonium based ILs. In fact, Silva *et al.* showed that a phosphonium IL combined with a bis 2,4,4-(trimethylpentyl)phosphinate anion was able to initiate the polymerization without any decomposition step [16] [17]. The authors suggested a nucleophilic attack from the phosphinate anion on the oxirane group, generating the alkoxide anion, required for the propagation. They highlighted a highly reactive system, requiring only a few amounts of IL (> 5 phr) in order to achieve a complete epoxy conversion. Thus, epoxy network was developed, exhibiting good mechanical performances and thermal stability with high glass transition temperatures (>140 °C for 10 phr of IL) compared to conventional epoxy-amine thermosets [16]. Maka *et al.* studied epoxy nanocomposites based on epoxy with the same IL as Silva *et al.*, i.e a phosphonium/phosphinate combination [18].

Thereafter, Nguyen *et al.* have compared epoxy network initiated with the same phosphonium IL denoted ILTMP and a phosphonium based IL including a diethyl phosphate counter-anion also able to initiate the epoxy polymerization. Although they have exhibited a high glass transition temperature (114 °C for 10 phr of tri(butyl)ethylphosphonium diethyl phosphate) with a better thermal stability than an epoxy-amine system, they remained less interesting due to their lower reactivity and final glass transition temperatures compared with the phosphinate anion based system [17].

Previous studies on electrical properties of epoxy/IL systems were mostly dedicated to electrolyte solutions. For this purpose, ILs were added : (i) as classic curing agents (in stoichiometric conditions with the epoxy prepolymer) [7] [19][19] [20]; (ii) in large excess leading to low glass transition temperatures [7] [19] [21]; (iii) or simply to another matrix than a polyepoxide one (more conventional for electrolytes, as PEO) [6]. Finally, dielectric properties and conduction mechanisms were not especially investigated after an anionic homopolymerization, for which the IL is involved in the curing process.

The present study investigates the dielectric behaviour of epoxy/IL systems according to the network properties obtained after the anionic homopolymerization. The curing process was investigated by DSC measurements for different contents of IL. The morphology of the network was also studied by TEM and related with DMA measurements. Finally, the dielectric measurements were performed by dielectric spectroscopy. For the first time, all the results were compared to a conventional epoxy/anhydride system.

2 EXPERIMENTAL

2.1 MATERIALS

An epoxy prepolymer based on diglycidyl ether of bisphenol A (DGEBA) was purchased from Huntsman (Araldite CY 225). A methyl-tetrahydrophthalic anhydride (MTHPA) hardener was also provided by Huntsman (Aradur HY 925) and used as comparison in stoichiometric conditions (80 phr, *phr: per hundred resin*). An imidazole based catalyst is also present in the anhydride formulation. The ionic liquid (IL) denoted ILTMP was supplied by Solvay (Cytac® IL104) and is made up of a trihexyl(tetradecyl)phosphonium cation, associated with a bis 2,4,4-(trimethylpentyl)phosphinate anion. The Table 1 summarizes the structure and characteristics of the used materials.

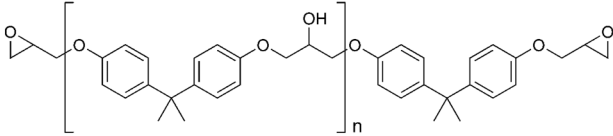
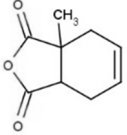
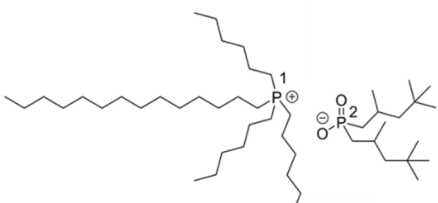
Name	Structure	Characteristics
DGEBA		$n = 0.2$
MTHPA		$M = 166 \text{ g.mol}^{-1}$
ILTMP		$M = 772 \text{ g.mol}^{-1}$

Table 1 : Chemical structures and properties of used compounds.

2.2 PROCESSING OF THE EPOXY NETWORKS

Different amounts of ionic liquid (4-20 phr) and anhydride (20-120 phr) were added to the neat epoxy prepolymer. All the blends were mixed during 10 min under vacuum at room temperature, in a planetary mixer (DAC 800 model from FlackTek Inc.). Then the formulations were cured in a stainless steelmould covered with a release agent (to avoid adhesion of the sample to the mould) at 100 °C during 4h and 140°C during 8h. The final samples were maintained in a dried atmosphere (in desiccator) until their characterization. Results were compared to a conventional epoxy/anhydride system, prepared following the same protocol.

2.3 CHARACTERIZATIONS

Differential scanning calorimetry (DSC) analyses were performed in a Q10 calorimeter from TA Instruments, at 10 °C/min from -80 to 300 °C under nitrogen flow. Samples (uncured blends) of 3-5 mg were sealed in hermetic aluminium pans. The energy corresponding to polymerization reaction was obtained by integrating the exothermic peak from a first ramp of temperature. A second ramp was applied in order to verify that all of the curing process has been done during the first step. Initial and final glass transition temperatures (respectively T_{g1} and T_{g2}) have also been collected.

As the samples were stored in a desiccator, all characterizations were carried out on dried samples.

Fourier Transform Infrared absorption spectra (FTIR-ATR) were obtained using a Thermo Scientific Nicolet iS10 spectrometer in a reflexion mode from 4000 to 650 cm^{-1} (32 scans per sample, 4 cm^{-1} resolution).

Transmission Electron Microscopy (TEM) was performed using a Phillips CM120 microscope (accelerating voltage up to 80 kV). 60-nm-thick samples were cut by ultramicrotome with a diamond knife and set on copper grids.

Dynamic mechanical thermal analysis (DMA) was undertaken using a Mettler Toledo system (SDTA 861e). Tests were carried out from 25 to 230 °C (3 °C/min) with a tensile strain of 3% applied at a frequency of 1 Hz.

Dielectric Analysis (DEA) was carried out using an XM Ametek Solartron spectrometer, in a sample cell and a cryogenic system provided by the Janis Research Company. Characterized samples are disk-shaped with a thickness of 1 mm. Gold electrodes were sputtered on both sides to ensure good electrical contacts. The diameter of the electrodes is equal to 25 mm. A voltage of +/- 5 V was applied at a frequency from 1 MHz to 0.1 Hz and a temperature range from -100 to 200 °C (isothermal step every 3 °C). Relative permittivity and dielectric loss were evaluated, as well as the real part of the conductivity and the equivalent DC conductivity from the low frequencies at high temperature. The DC conductivity σ_{DC} was calculated from the low frequency plateau of the real part σ' of the complex conductivity, defined as:

$$\sigma'_{AC} = \omega \varepsilon'' \quad (1)$$

Where ω and ε'' are respectively the angular frequency ($\omega = 2\pi f$, with f the frequency) and the imaginary part of the complex permittivity.

The dielectric relaxation modes were analysed by using a Cole-Cole model, expressed by the equation (2).

$$\varepsilon^*(\omega) = \varepsilon_{\infty} + \frac{\Delta\varepsilon}{1 + (j\omega\tau)^{\alpha}} \quad (2)$$

With α the shape parameter describing the symmetric broadening of the relaxation peak, τ the relaxation time at the angular frequency ω , and $\Delta\varepsilon = \varepsilon_s - \varepsilon_{\infty}$ with ε_{∞} and ε_s respectively the infinite and static permittivities.

The fragility index was defined by Angell *et al.* [22] and is calculated from equation (4). The fragility index m allows to classify as “strong” (low m value and Arrhenius-like behaviour or “fragile” (higher value of m and deviation from the Arrhenius behaviour):

$$m = \left. \frac{d(\log \tau)}{d(T_g/T)} \right|_{T=T_g} \quad (3)$$

3 RESULTS AND DISCUSSION

3.1 CURING BEHAVIOUR OF EPOXY/IL SYSTEMS

The curing process of epoxy/IL systems was followed by DSC measurements. Unlike conventional hardeners, the IL does not form a bridge between epoxy macromolecules, but acts as an initiator of an anionic homopolymerization (the IL anion will stand chemically linked to the epoxy network after the polymerization) [16]. Figure 1 shows the heat flow corresponding to the exothermic reaction of the epoxy anionic homopolymerization induced by the IL. Characteristic temperatures and exothermic enthalpies are summarized in Table 2.

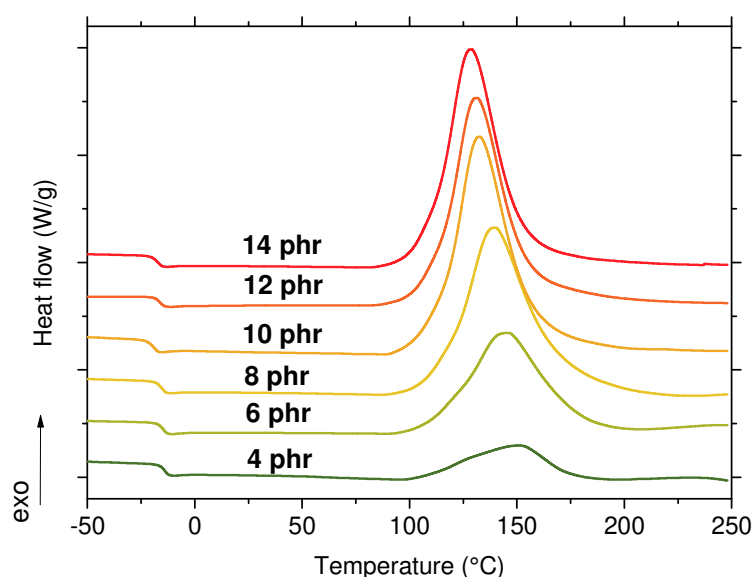


Figure 1: DSC thermograms of epoxy/IL systems for different contents of IL.

Whatever the concentration of IL, an exothermic peak representative of polymerization appeared. Associated enthalpy ΔH increases with the increase of the IL content and reaches a maximum of 81 kJ/epoxy equivalent (388 J/g) for 10 phr of LI, which appears to be the optimal ratio required to achieve a full polymerization. This content also leads to the highest glass transition temperature (110 °C), suggesting that the excess of IL will not take part in the polymerization process for IL contents higher than 10 phr but will act as a plasticizer decreasing the glass transition temperature [17]. The second temperature ramp does not show a residual exothermic peak. The highest temperature of the T_{g2} glass transition (110 °C) is also obtained for 10 phr, values in agreement with the literature [16] [17] [18] [23]. No glass transition temperature has been detected for 4 and 6 phr of LI suggesting an incomplete polymerization, due to the lack of LI in the reactive mixture.

Table 2: Characteristic temperatures, and exothermic energies depending on the IL content.

ILTMP content (phr)	Onset temperature (°C)	Peak temperature (°C)	ΔH (J/g)	ΔH (kJ/ee)	T_{g2} (°C)
4	106	151	82	16	-
6	105	146	229	46	-
8	104	140	364	75	99
10	111	136	388	81	110
12	102	131	369	79	103
14	98	129	372	81	96
20	103	142	342	78	95
Anhydride (80 phr)	130	167	297	102	95

The decrease of the onset temperature can be attributed to the initiation of the homopolymerization from the phosphinate anion as well as the initiator effect of the phosphonium cation. Indeed, Smith *et al.* highlighted the ability of phosphonium based compounds to act as latent accelerator of the epoxy polymerization [24]. They suggested the formation of active species from hydrogen bonded phosphonium/epoxy complexes.

In optimum conditions, the IL leads to a more reactive system than the anhydride, exhibiting a lower onset temperature (111 and 130 °C for respectively 10 phr of IL and 80 phr of anhydride), as well as a higher exothermic heat (366 and 297 J/g for respectively 10 phr of IL and 80 phr of anhydride). As a conclusion, DSC results highlighted the ability of the IL to be used as an initiator of the homopolymerization as it was previously suggested in the literature. An optimum content was established around 10 phr, above which a plasticizing effect due to the IL excess appears.

3.2 MORPHOLOGY OF EPOXY/IL NETWORKS

The morphologies of epoxy networks containing ILTMP were evaluated by TEM and presented in Figure 2 for different contents of IL (6, 12 and 20 phr). Clusters probably due to IL agglomeration are observed for 6 and 12 phr of IL. These observations are confirmed in several works highlighting the ability of ILs to generate a phase-separated morphology into thermosets or thermoplastic matrices when the miscibility threshold is exceeded [23] [25]. A phase separation phenomenon or large IL rich zones are observed for 20 phr: the darkest phase can be probably attributed to a highly IL-concentrated phase coming from the excess of IL which did not take part in the polymerization process.

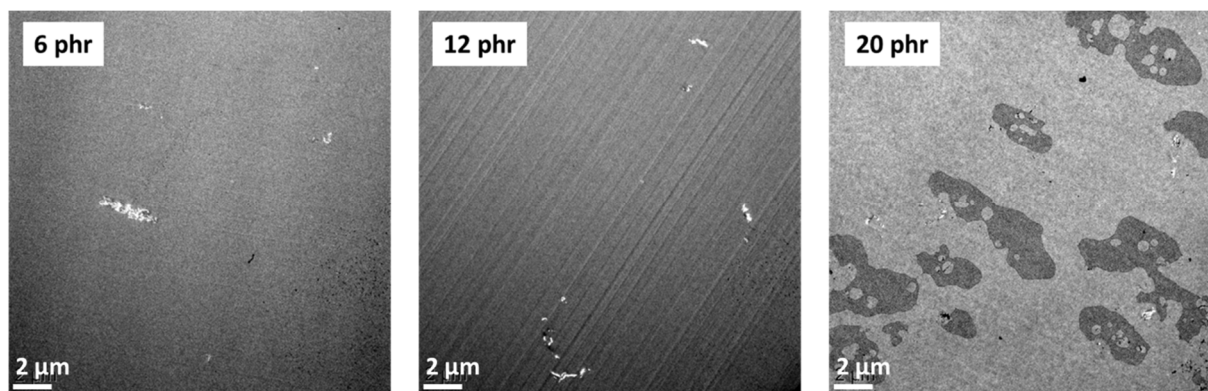


Figure 2: TEM observation of epoxy systems for different contents of ILTMP.

From dynamic mechanical measurements on all epoxy networks with and without ILTMP, Figure 3 and Figure 4(A), display the storage modulus E' , loss modulus E'' and dissipation factor $\tan \delta$ as a function of temperature. Table 3 summarizes the main relaxation temperature T_α associated with the glass transition and the cooperative movement of macromolecular chains observed on the $\tan \delta$ curve (Figure 4 (A)) and the rubbery modulus E'_R .

The plateau obtained at high temperature on the storage modulus, corresponding to the rubbery modulus, is drastically increased for epoxy/IL systems (154 and 20 MPa for respectively 8 phr of IL and 80 phr of anhydride), suggesting a higher crosslink density of epoxy/IL systems due to the homopolymerization.

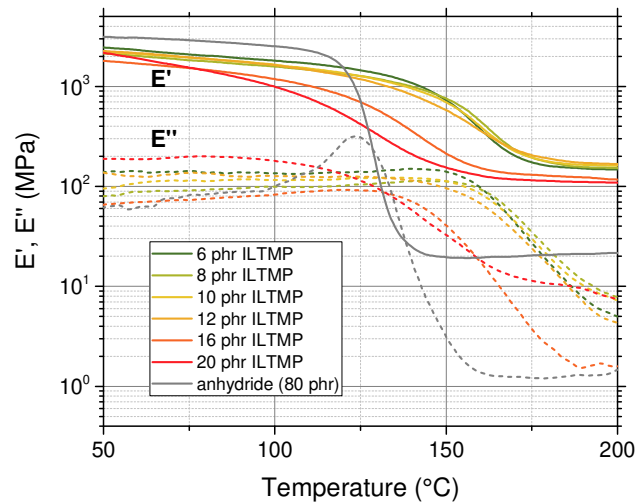


Figure 3: Storage modulus and loss modulus as a function of temperature for different contents of IL compared to the epoxy/anhydride system.

Epoxy/IL systems exhibit high α relaxation peak temperatures (> 160 °C between 6 and 12 phr) with a maximum of 165 °C achieved for 8 phr of IL. This content is different from DSC measurements for which a maximum glass transition (2nd ramp) was obtained for 10 phr. Indeed, the DSC ramp from -100 to 200 °C (10 °C/min) is not representative of the real curing process applied in oven. Whatever, the optimized content must be between 8 and 10 phr of IL.

Table 3: Thermomechanical behaviour of epoxy networks cured with IL.

ILTMP content (phr)	T_{α} (°C)	E'_R (MPa)
6	160	151
8	165	154
10	162	164
12	159	173
16	144	131
20	132	125
Anhydride (80 phr)	132	20

While keeping a high rubbery modulus whatever the IL content, the α relaxation peak temperature T_{α} is drastically decreased as the IL content increases (from 162 to 132 °C for respectively 10 and 20 phr). As previously observed by DSC, the IL leads to a plasticizing effect since the IL excess do not take part in the polymerization process. The excess of IL causes a wider relaxation peak, illustrated by the normalization of the relaxation peak as a function of its amplitude and temperature in Figure 4 (B). The epoxy network heterogeneity increases with the IL content, result supported by the heterogeneities previously observed by TEM (clusters apparition whose size depends on the IL content).

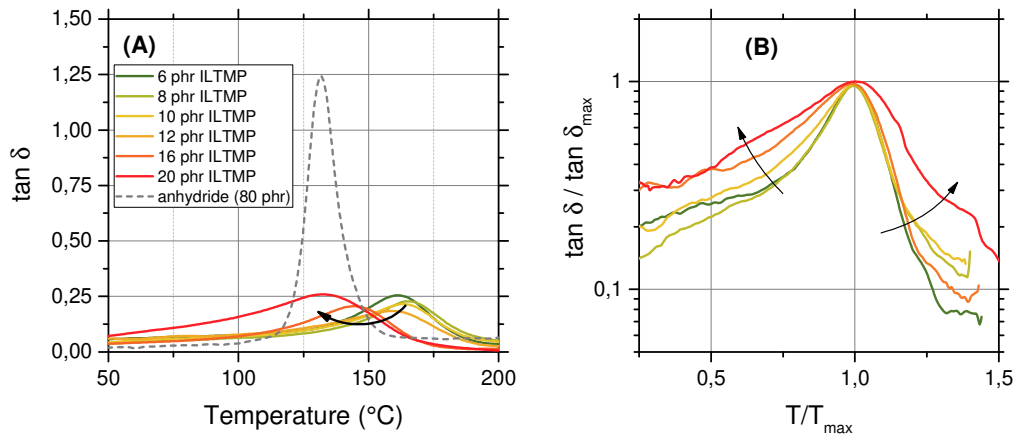


Figure 4: (A) Loss tangent in function of temperature, (B) normalization of α relaxation peak.

DMA results highlight the ability of IL to generate stiff epoxy network displaying high glass transition temperature (≈ 160 °C). Nevertheless, IL excess drastically reduces the temperature of α relaxation due to its plasticizing effect. When the IL content increases, the broadening of the $\tan \delta$ peak proves the formation of a more and more heterogeneous environment around relaxing entities.

3.3 DIELECTRIC BEHAVIOUR OF EPOXY/IL NETWORKS

3.3.1 Relaxations analysis

Dielectric behaviour was investigated by dielectric spectroscopy. Figure 5 shows relative permittivity and dielectric loss as a function of temperature at 10 Hz. Several mechanisms appear:

- i. The localized mobility of branched molecular segments induces the β *relaxation mode* at low temperature. It is mainly associated to hydroxyether groups from the epoxy prepolymer chain [26] [27]. Its temperature at the maximum of $\tan \delta$ is close to the epoxy/anhydride system and does not seem to be modified by the IL content.
- ii. The α *relaxation mode* is the dielectric manifestation of the glass transition. It is associated with the cooperative and delocalized mobility of macromolecular chains. Although it clearly appears as a shoulder on dielectric loss for the epoxy/anhydride system, the α mode is not visible on dielectric loss for IL-containing samples. Indeed, this relaxation mode is hidden by conduction phenomenon occurring at high temperature.
- iii. *Conduction mechanisms* σ arise at high temperature and conceal the α relaxation on dielectric loss. It increases with the IL content.
- iv. A *relaxation mode called ω* is observed between the β and α relaxation modes for the highest contents of IL (16 and 20 phr ILTMP). This relaxation is not well understood and some authors attributed this relaxation to the dielectric manifestation of some heterogeneities in the network [28] [29]. This relaxation seems to be sensitive to water uptake in epoxy systems and associated with the motion of cyclohexyl units in epoxy-anhydride networks [30].

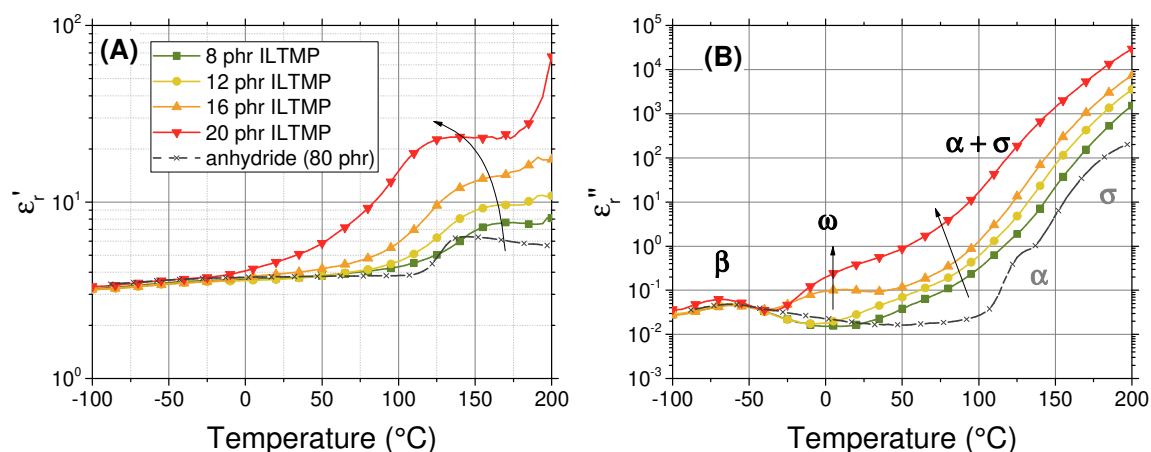


Figure 5: (A) Relative permittivity and (B) dielectric loss for different contents of IL, $f = 10$ Hz.

A Cole-Cole model was applied to the different relaxation modes. Arrhenius plot of relaxation time from α and β modes are shown in Figure 6.

a) α Relaxation

The frequency dependence of the relative permittivity and the dielectric losses between 80 and 200 °C for 10 and 20 phr IL is shown in *Supporting Information (Figure S1)*. A temperature jump in relative permittivity, associated with the α relaxation, is observed in Figure 5 and appears to be greater for 20 phr of IL. The large increase of permittivity at low frequency is due to the contribution of conduction, identified by a slope of (-1) on the dielectric losses.

The application of a Cole-Cole model added to the conduction slope makes it possible to discriminate the α relaxation from the conduction contribution on the dielectric loss. The parameters α and $\Delta\epsilon$ are reported in *Supporting Information (Table S1 and Figure S3)*. The α parameter, characteristic of the distribution width of the relaxation time, is usually independent on temperature [31]. The width of the distribution does not appear to vary with the amount of IL (about 0.40). However, the α relaxation is broader than one of the stoichiometric system epoxy/anhydride (about 0.50). These results are in agreement with the dynamic mechanical analysis, for which a wider α relaxation peak is also observed for epoxy/LI systems (Figure 4).

The $\Delta\epsilon$ factor and its temperature dependence increase with the amount of IL. A strong dependence is observed for 20 phr of IL, with a permittivity jump greater than 20. This increased temperature dependence when the amount of LI increases matches with the relative permittivity jump observed in Figure 5. The $\Delta\epsilon$ factor of the Cole-Cole model is proportional to the number of dipoles involved in the relaxation process [31]. It is therefore sensitive to the concentration, the nature and the environment of these dipoles. The increase of the $\Delta\epsilon$ factor is consistent with an increase of the network mobility in the presence of IL as the number of available dipoles increased with the IL content. At a given temperature, this mobility is also shown in Figure 6 (A) by a decrease of relaxation time when the IL content increases (or by a time shift towards low temperatures). The temperature dependence of the $\Delta\epsilon$ parameter, which is increased as the amount of IL increases (significantly decreased from 37 to 23 between 110 and 144 °C for 20 phr), could be explained by the intervention of conduction mechanisms in which the dipoles associated with the relaxation mode α would be involved. Therefore, they would no longer contribute to the permittivity jump.

The relaxation time of the α relaxation in Figure 6 (A) are higher for epoxy/IL networks than the epoxy/anhydride one. It is due to the homopolymerization generating a network with a high crosslink density, and, thus, a low chain mobility compared to epoxy/anhydride copolymerized network. The discussion will focus on this point. The results from the VFT law applied for 8 and 20 phr are shown in *Supporting Information (Table S2)*. The T_V temperatures deviate slightly from the $T_g - T_V = 50^\circ\text{C}$ case commonly observed for polymers and for the epoxy/anhydride system proposed in this study. Parameter D is characteristic of the deviation from a VFT law to an Arrhenius law (respectively from a “fragile” to “strong” behaviour). In the present case, it appears to be sufficiently low (close to 1) to express a VFT behaviour. On the other hand, the fragility index m of the epoxy/IL systems is much lower than the epoxy/anhydride system (respectively 30 and 64). According to Angell’s argumentation, it seems to indicate epoxy/IL are “stronger” which seems to be inconsistent with the value of D [22]. Calorimetric measurements and the Donth approach based on the Adam and Gibbs theory could be interesting to determine the cooperativity length [32] [33].

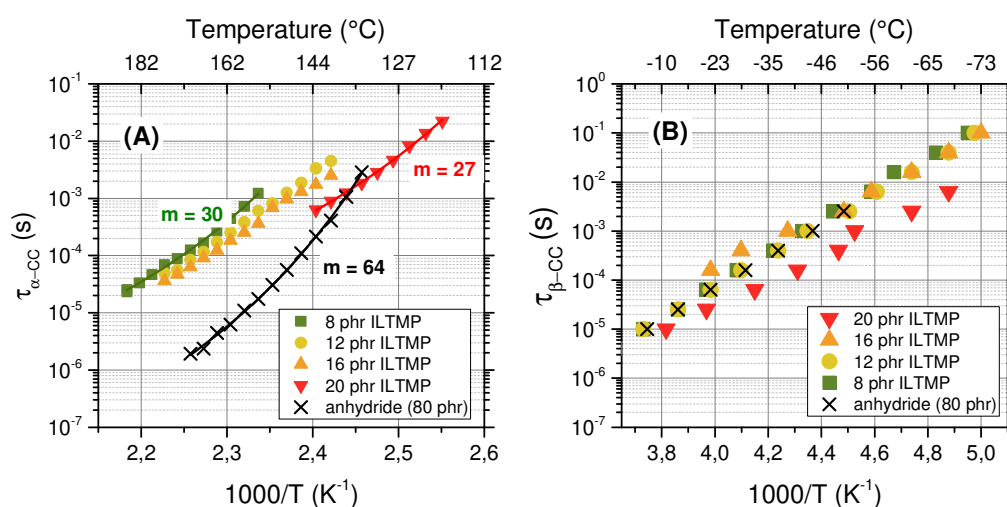


Figure 6: Arrhenius plots of relaxation time for (A) the α relaxation mode (lines correspond to a VFT law application), and (B) the β relaxation mode.

b) β relaxation

Relaxation time from β mode is plotted in Figure 6 (B). The temperature dependence of the relaxation time of epoxy/IL systems appears to be close to the conventional epoxy/anhydride and suggests a similar contribution of the hydroxyether groups. The parameters derived from Arrhenius law are shown in Table 4. According to the Arrhenius law, a decrease of the activation energy with the IL content appears from 0.66 to 0.53 eV for respectively 8 and 20 phr of IL-TMP, common value observed for sub glass relaxation. An activation energy value close to the epoxy/anhydride system is obtained for small amounts of IL (8 phr). The contribution of the lateral groups thus appears similar and not altered when the IL is not in excess. When there is an excess of IL, the higher mobility of the P=O groups associated with free anions could explain an additional contribution and the decrease of the activation energy when the IL amount increases.

Table 4: Activation energies from β relaxation mode.

ILTMP content (phr)	$E_{A-\beta}$ (eV)
8	0.66
10	0.63
12	0.62
16	0.57
20	0.53
Anhydride (80 phr)	0.69

c) ω relaxation

The ω relaxation mode is only observed for high content of IL (16 and 20 phr). Due to multiple and complex overlaps obtained for 20 phr, only results for 16 phr of IL were available for data processing. The relative permittivity as a function of temperature is shown in Figure 7 (A) at different frequencies. This relaxation mode occurs for temperatures between the β and α modes (Figure 7 (B)). Its activation energy was calculated from an Arrhenius law and estimated at 0.67 eV. This value is similar to the activation energies obtained in Table 4 for the β relaxation mode of the epoxy/IL and epoxy/anhydride systems (respectively 0.66 eV for 8 phr ILTMP and 0.69 eV for the anhydride) and, thus, suggests mechanisms close to the sub glass relaxation process, *i.e.* localized dipoles involved in the relaxation. This relaxation may be attributed to the previously observed heterogeneities and will be discussed from this point of view.

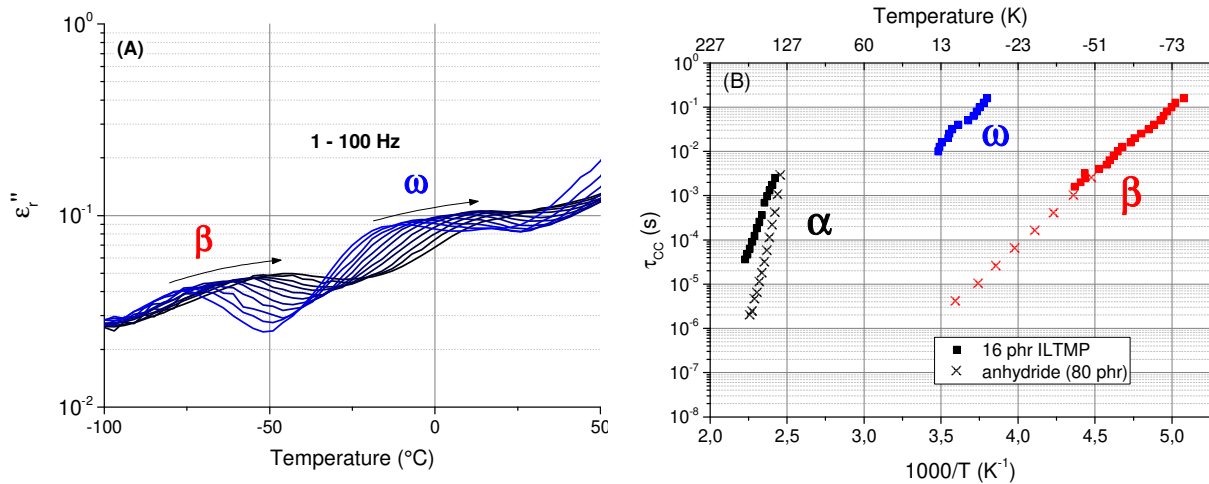


Figure 7: (A) β and ω relaxation modes for different frequencies between 1 and 100 Hz (indicated by the arrow from low to high frequencies) for 16 phr ILTMP, and (B) Arrhenius plots of all relaxation modes for 16 phr ILTMP, compared to the epoxy/anhydride system.

3.3.2 Electrical conductivity

The real part σ'_{AC} of the complex conductivity is shown in Figure 8 between 80 and 170 $^{\circ}\text{C}$ for different contents of IL. A DC conduction plateau is observed at low frequency for all formulations. The DC plateau appears for temperatures lower than T_{α} previously reported. A steady plateau is obtained from 110 $^{\circ}\text{C}$ at 0.1 Hz for 8 phr of IL while the corresponding T_{α} is equal to 162 $^{\circ}\text{C}$. Thus, it means that conduction mechanism occurs at low temperature even below the glass transition.

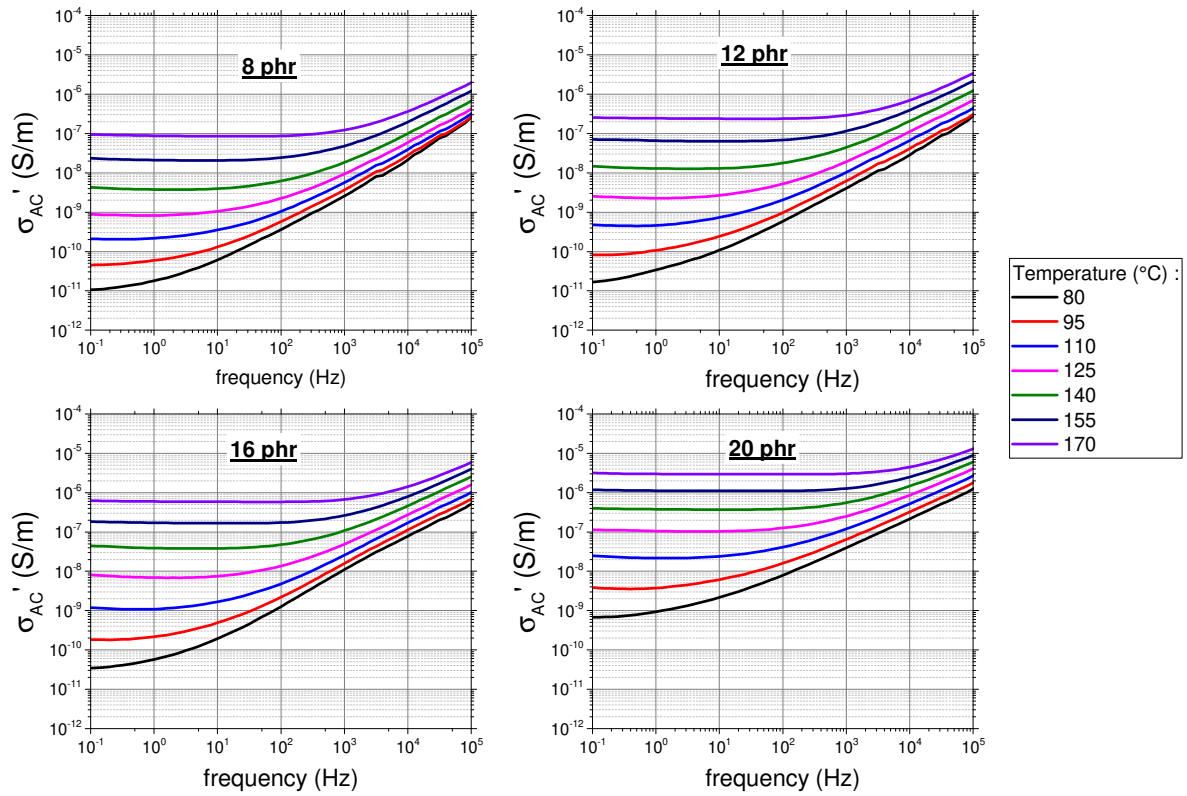


Figure 8: AC conductivity from dielectric spectroscopy for different contents of ILTMP.

The Arrhenius plot of the DC conductivity calculated from equation (2) is presented in Figure 9 for different contents of IL and compared to the epoxy/anhydride system. The DC conductivity is increased by one order of magnitude on the whole range of temperature when the anhydride hardener is substituted by 12 phr of IL-TMP, and increased by two orders of magnitude or more with the substitution by 20 phr of IL.

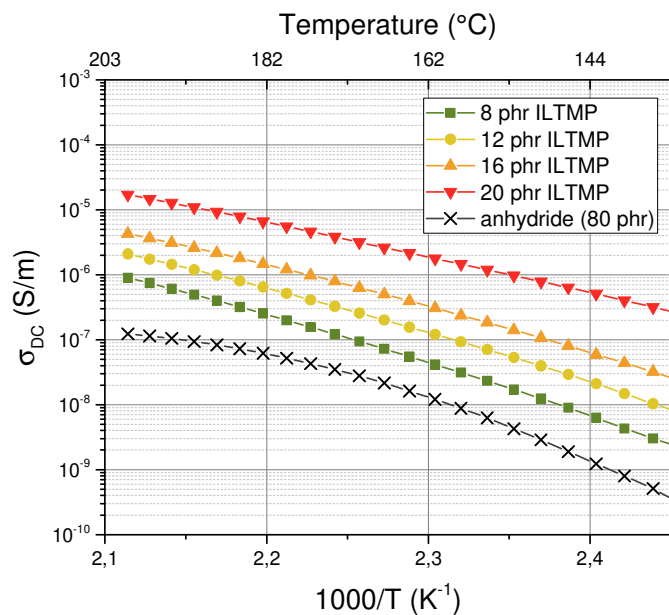


Figure 9: Arrhenius plot of the DC conductivity from dielectric spectroscopy.

DC conductivity in polymers is usually fitted by a VFT law defined by equation (5) [34] [35].

$$\sigma_{VFT} = \sigma_0 e^{-DT_V/(T-T_V)} \quad (4)$$

With σ_0 a pre-exponential factor, D a strength parameter quantifying the deviation from the VFT law toward Arrhenius, T_V the Vogel temperature, and T the temperature. This expression from Adams-Gibbs theory suggests an activation mechanism principally led by segmental mobility of the polymer host, *i.e.* depending on the glass transition (with T_V usually considered as $[T_g - 50^\circ\text{C}]$). The VFT parameters as a function of IL content are reported in *Supporting Information (Table S3)*. Unlike the epoxy/anhydride system, the curvature of DC conductivity from epoxy/IL networks does not illustrate a VFT behaviour. It is confirmed by the high values of D parameters, indicating a deviation from the VFT law towards an Arrhenius behaviour. Consequently, T_V values are senseless and far lower from $[T_g-50^\circ\text{C}]$. One could immediately think that the curvature loss would come from a VFT law shifted towards higher temperatures, due to higher glass transition temperatures of epoxy/IL networks. Nevertheless, the α temperature for 20 phr of IL is about 132°C , which is equal to the α temperature of the epoxy/anhydride system. Thus, another explanation will be proposed and discussed later.

3.4 DISCUSSION

An optimized epoxy/IL network seems to be obtained by adding between 8 and 10 phr of IL, for which the highest reaction enthalpy and glass transition temperature were reported by DSC and DMA. The theory of rubber elasticity can't be strictly applied on the rubbery modulus since the original theory is based on several hypothesis which are not totally fulfilled in epoxy/IL systems [36]. Moreover, its validity is linked to the study of homogeneous systems, which is not the case for the highest IL contents exhibiting a separation phase. However, the increase of the rubbery modulus can be associated with the high crosslink density of the network and/or to additional interactions involved in the epoxy/IL systems compared to the epoxy/anhydride one. A simple calculation of the theoretical mass between crosslinks is proposed in *Supporting Information (Figure S5)*, according to the initiation and propagation schemes presented in Figure 10. Mass between crosslinks of 184 g.mol^{-1} and 267 g.mol^{-1} were calculated for respectively 10 phr of IL and 80 phr of anhydride, which is correlated with the increase of the rubbery modulus.

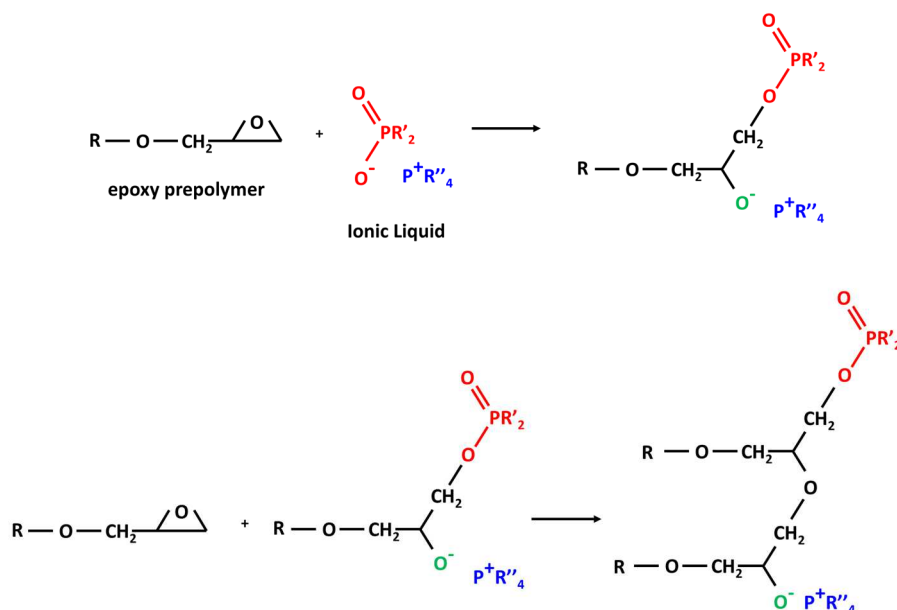


Figure 10: Initiation and propagation of the epoxy homopolymerization: the successive reactions of epoxy groups generates ether segments explaining the high crosslink density compared to classical epoxy/anhydride network.

As a conclusion from DSC and DMA results, a 2D network architecture can be proposed in Figure 11. Two points are highlighted in this simplified illustration: (i) the high cross-linking density, and consequently the large number of cross-linking points; (ii) the position and steric hindrance of the IL (approximate size scale of cations and anions relative to the prepolymer). The low mass between crosslinks calculated from the epoxy/IL system could be explained by the contribution of -O-CH₂-sequences generated between crosslinks by the propagation step of the homopolymerization [37] (Figure 10).

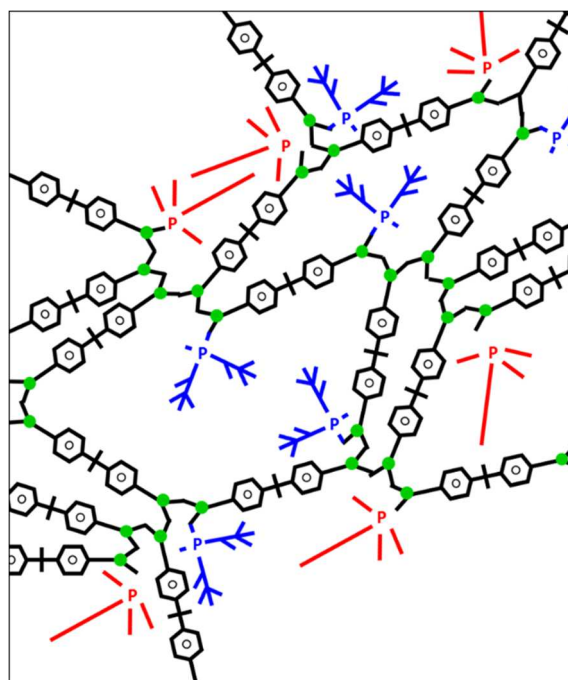


Figure 11: 2D representation of an epoxy network induced by anionic homopolymerization in presence of IL: (blue) IL anion, (red) IL cation, (black) prepolymer; (green) crosslinks.

Several phenomena were observed and associated with dielectric relaxation modes of epoxy/IL networks:

- An increase with IL content of the chain mobility involved in the α relaxation process, principally due to a plasticizing effect induced by the excess of IL from the polymerization process. On the other side, a “strong” behaviour has been identified according to the Angell’s argumentation (low fragility index). It is in agreement with results from conductivity which does not seem to depend on segmental mobility.
- The activation of the β relaxation mode is enhanced by the presence of IL. It could be due to the steric hindrance of the IL near the hydroxyether groups involved in the relaxation process. P=O dipoles from the IL would also contribute to this relaxation mode.
- A ω relaxation mode is observed between the α and β relaxations. It is similar to the most known but controversy ω relaxation observed in several studies [38] [39] [40] [29]. Indeed, authors were able to associate it with various mechanisms: the heterogeneity of the network, the presence of moisture, or the mobility of aromatic nuclei or of hydroxyether groups. In the present study, the water absorption may probably not be the cause due to the sample storage in dried atmosphere. Activation energies indicate a dielectric relaxation close to sub glass relaxations, *i.e.* associated with hydroxyl dipoles orientation. In order to broaden the discussion, FTIR measurements were performed in the wavelength range corresponding to hydroxyl groups (3000-3700 cm^{-1}). An additional contribution seems to appear at 3300 cm^{-1} when the amount of IL increases. The involvement of -OH groups of epoxy network in interactions with IL could be responsible for this absorption peak [41]. However, their involvement is not trivial, since the absorption peak is also observed for the neat IL. It could therefore be attributed to intrinsic cation/anion interactions of the IL. Consequently, we tend to explain the increase in amplitude of the ω relaxation. We assume that the network is more and more heterogeneous as the IL content increases. The broadening of the $\tan \delta$ proves it. Previous works tends to demonstrate that the presence of ω relaxation can be due to the absorption of small amount of water inside the network generating heterogeneities in the network where the molecular mobility is higher in these zones (mobility of cyclohexyl units for example). By analogy, we can make the hypothesis that IL promotes the mobility of small units like cyclohexyl ones leading to this ω relaxation on dielectric measurements. FTIR measurements could confirm this result showing the existence of cation/anion interactions. We discard the hypothesis of water absorption for two reasons : first, dielectric measurements were done on dried samples and the second temperature run still exhibits the relaxation and second, the IL introduced into the network is hydrophobic as much as the network itself (energy surface measurements confirmed this result).

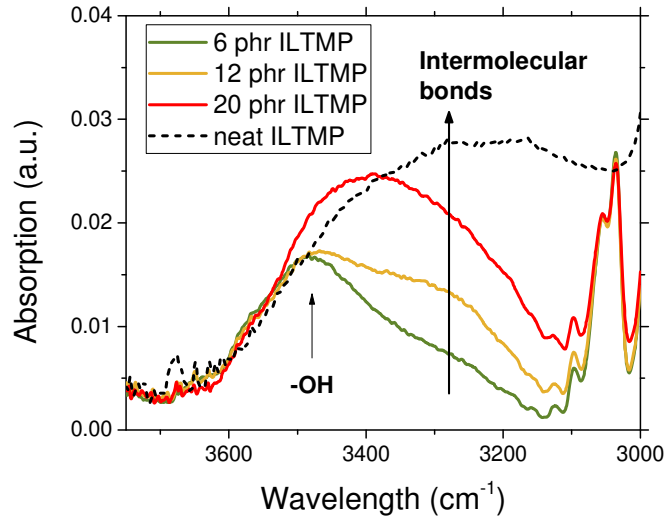


Figure 12: FTIR-ATR analysis for different ILTMP

DC conductivity analysis have shown that conduction phenomena occurred far below the glass transition temperature of epoxy/IL networks. Moreover, the temperature behaviour of the conductivity of these new systems does not follow a traditional VFT behaviour. A thermal activation mechanism has to be considered by the application of an Arrhenius law, defined by the equation (6).

$$\sigma_{Arrh} = \sigma_0 e^{-E_A/k_B T} \quad (6)$$

The corresponding Arrhenius parameters are reported in Table 5. The activation energy E_A decreased with the addition of IL. The activation energies, higher than 1, probably indicate a conduction process essentially led by ionic conduction [42]. Nevertheless, the charge carrier identification is not trivial:

- At first sight, it would be easy to identify the *ionic contribution essentially coming from the mobility of the IL* (cation and/or anion). But the ions molecular weight (respectively 483 and 289 g.mol⁻¹ for the cation and anion) are similar to the prepolymer molecular weight. Their 3D representations are shown in *Supporting Information (Figure S6)*. Moreover, these masses are of the same order of magnitude as the approximated mass between crosslinks previously calculated. Consequently, IL mobility may be complicated in such highly crosslinked epoxy networks.
- A *contribution of proton conduction* is an option since hydroxyl groups are initially found in the epoxy prepolymer [43].
- *Ionic impurities* coming from the DGEBA or IL preparation would also contribute to ionic conduction process [44].

Table 5: Parameters of the Arrhenius law applied to DC conductivity for different contents of IL.

ILTMP content (phr)	σ_0 (S/m)	E_A (eV)
8	$7.3 \cdot 10^9$	1.49
10	$2.9 \cdot 10^9$	1.45
12	$1.2 \cdot 10^9$	1.38
16	$2.5 \cdot 10^8$	1.29
20	$3.2 \cdot 10^6$	1.06

Finally, the IL mobility is probably not the main contribution to the DC conductivity. It would more probably act as a promotor of ionic conduction (proton and small ionic impurities) due to: (i) its plasticizing effect, increasing the network mobility in the range of the glass transition temperature and for higher temperatures; (ii) the orientation of IL's ionic interactions, favouring the conducting ions towards the electric field.

4 CONCLUSION

The substitution of conventional hardeners by ionic liquids has a significant influence on the epoxy polymerization process, the network and its final solid properties. Previous studies highlighted the ability of IL to initiate an epoxy homopolymerization. In this study, strong relationships have been established between the epoxy network morphology and, for the first time, its dielectric behaviour. The main results and conclusions of this work are: (i) an increase of the macromolecular mobility due to the IL excess; (ii) the emergence of a ω relaxation mode identified as the dielectric manifestation of heterogeneities of the network generated by the excess of IL in the network; (iii) a significant increase of the DC conductivity until 2 decades higher than a conventional epoxy/anhydride system, and obtained from temperatures much lower than the glass transition; (iv) a thermal activation mechanism of the ionic conduction defined by an Arrhenius behaviour. The present study highlighted the potential of epoxy/IL system for insulation application requiring an interesting electric conductivity even below the glass transition temperature (for example to reduce static charge accumulation) while maintaining excellent solid properties, with a high crosslink density combined to a high glass transition temperature ($T_g > 160$ °C). This innovative route can be also considered in order to enhance electrical conductivity below the glass temperature.

5 ACKNOWLEDGEMENTS

The authors acknowledge Pierre Alcouffe and the Consortium Lyon Saint-Etienne de Microscopie (CLYM, FED 4092) for the access to the microscopes.

This work was supported by a grant overseen by the French National Research Agency (ANR) as part of the "Investissements d'Avenir" Program (ANE-ITE-002-01)

This manuscript is in honor of the 50 year anniversary of the French Polymer Group (Groupe Français des Polymères – GFP).

This work is also dedicated to Professor Jean-Pierre PASCAULT, famous scientist of thermosetting polymers. He was a friend of ours.

6 REFERENCES

- [1] J. Vila, P. Ginés, J. M. Pico, C. Franjo, E. Jiménez, L. M. Varela and O. Cabeza, "Temperature dependence of the electrical conductivity in EMIM-based ionic liquids: Evidence of Vogel–Tamman–Fulcher behavior," *Fluid Phase Equilibria*, vol. 242, pp. 141-146, 2006.
- [2] O. Zech, A. Stoppa, R. Buchner and W. Kunz, "The Conductivity of Imidazolium-Based Ionic Liquids from (248 to 468) K. B. Variation of the Anion," *Journal of Chemical & Engineering Data*, vol. 55, pp. 1774-1778, 2010.
- [3] H. Ohno, M. Yoshizawa and W. Ogihara, "Development of new class of ion conductive polymers based on ionic liquids," *Electrochimica Acta*, vol. 50, pp. 255-261, 2004.
- [4] M. Galiński, A. Lewandowski and I. Stępnia, "Ionic liquids as electrolytes," *Electrochimica Acta*, vol. 51, pp. 5567-5580, 2006.
- [5] S. K. Chaurasia and R. K. Singh, "Electrical conductivity studies on composite polymer electrolyte based on ionic liquid," *Phase Transitions*, vol. 83, pp. 457-466, 2010.
- [6] A. Tsurumaki, J. Kagimoto and H. Ohno, "Properties of polymer electrolytes composed of poly(ethylene oxide) and ionic liquids according to hard and soft acids and bases theory," *Polymers for Advanced Technologies*, vol. 22, pp. 1223-1228, 2011.
- [7] N. Shirshova, A. Bismarck, S. Carreyette, Q. P. V. Fontana, E. S. Greenhalgh, P. Jacobsson, P. Johansson, M. J. Marczewski, G. Kalinka, A. R. J. Kucernak, J. Scheers, M. S. P. Shaffer, J. H. G. Steinke and M. Wienrich, "Structural supercapacitor electrolytes based on bicontinuous ionic liquid–epoxy resin systems," *J. Mater. Chem. A*, vol. 1, pp. 15300-15309, 2013.
- [8] M.-D. Bermúdez, A.-E. Jiménez, J. Sanes and F.-J. Carrión, "Ionic Liquids as Advanced Lubricant Fluids," *Molecules*, vol. 14, pp. 2888-2908, 2009.
- [9] I. Minami, T. Inada, R. Sasaki and H. Nanao, "Tribo-Chemistry of Phosphonium-Derived Ionic Liquids," *Tribology Letters*, vol. 40, pp. 225-235, Nov 2010.
- [10] A. E. Somers, P. C. Howlett, D. R. MacFarlane and M. Forsyth, "A Review of Ionic Liquid Lubricants," *Lubricants*, vol. 1, pp. 3-21, 2013.
- [11] S. Livi, J.-F. Gérard and J. Duchet-Rumeau, "Ionic Liquids as Polymer Additives," in *Applications of Ionic Liquids in Polymer Science and Technology*, D. Mecerreyes, Ed., Berlin, Heidelberg: Springer Berlin Heidelberg, 2015, pp. 1-21.
- [12] S. Livi, J. Duchet-Rumeau, J.-F. Gérard and T. N. Pham, "Polymers and Ionic Liquids: A Successful Wedding," *Macromolecular Chemistry and Physics*, vol. 216, pp. 359-368, 2015.
- [13] H. Maka, T. Szychaj and R. Pilawka, "Epoxy Resin/Ionic Liquid Systems: The Influence of Imidazolium Cation Size and Anion Type on Reactivity and Thermomechanical Properties," *Industrial & Engineering Chemistry Research*, vol. 51, pp. 5197-5206, 2012.

- [14] F. C. Binks, G. Cavalli, M. Henningsen, B. J. Howlin and I. Hamerton, "Investigating the mechanism through which ionic liquids initiate the polymerisation of epoxy resins," *Polymer*, vol. 139, pp. 163-176, 2018.
- [15] A. Vashchuk, A. M. Fainleib, O. Starostenko and D. Grande, "Application of ionic liquids in thermosetting polymers: Epoxy and cyanate ester resins.," *Express Polymer Letters*, vol. 12, 2018.
- [16] A. A. Silva, S. Livi, D. B. Netto, B. G. Soares, J. Duchet and J.-F. Gérard, "New epoxy systems based on ionic liquid," *Polymer*, vol. 54, pp. 2123-2129, 2013.
- [17] T. K. L. Nguyen, S. Livi, S. Pruvost, B. G. Soares and J. Duchet-Rumeau, "Ionic liquids as reactive additives for the preparation and modification of epoxy networks," *Journal of Polymer Science Part A: Polymer Chemistry*, vol. 52, pp. 3463-3471, 2014.
- [18] H. Maka, T. Spychaj and R. Pilawka, "Epoxy resin/phosphonium ionic liquid/carbon nanofiller systems: Chemorheology and properties.," *Express Polymer Letters*, vol. 8, 2014.
- [19] M. Leclère, S. Livi, M. Maréchal, L. Picard and J. Duchet-Rumeau, "The properties of new epoxy networks swollen with ionic liquids," *RSC Adv.*, vol. 6, pp. 56193-56204, 2016.
- [20] K. Matsumoto and T. Endo, "Design and synthesis of ionic-conductive epoxy-based networked polymers," *Reactive and Functional Polymers*, vol. 73, pp. 278-282, 2013.
- [21] K. Matsumoto and T. Endo, "Confinement of ionic liquid by networked polymers based on multifunctional epoxy resins," *Macromolecules*, vol. 41, pp. 6981-6986, 2008.
- [22] R. Böhmer, K. L. Ngai, C. A. Angell and D. J. Plazek, "Nonexponential relaxations in strong and fragile glass formers," *The Journal of Chemical Physics*, vol. 99, pp. 4201-4209, 1993.
- [23] T. K. L. Nguyen, S. Livi, B. G. Soares, S. Pruvost, J. Duchet-Rumeau and J.-F. Gérard, "Ionic liquids: A New Route for the Design of Epoxy Networks," *ACS Sustainable Chemistry & Engineering*, vol. 4, pp. 481-490, 2016.
- [24] J. D. B. Smith, "Quaternary phosphonium compounds as latent accelerators for anhydride-cured epoxy resins. I. Latency and cure characteristics," *Journal of Applied Polymer Science*, vol. 23, pp. 1385-1396, 1979.
- [25] T. K. L. Nguyen, S. Livi, B. G. Soares, H. Benes, J.-F. Gérard and J. Duchet-Rumeau, "Toughening of Epoxy/Ionic Liquid Networks with Thermoplastics Based on Poly (2, 6-dimethyl-1, 4-phenylene ether)(PPE)," *ACS Sustainable Chemistry & Engineering*, vol. 5, pp. 1153-1164, 2016.
- [26] M. Chevalier, E. Dantras, C. Tonon, P. Guigue, C. Lacabanne, C. Puig and C. Durin, "Correlation between sub-T_g relaxation processes and mechanical behavior for different hydrothermal ageing conditions in epoxy assemblies," *Journal of applied polymer science*, vol. 115, pp. 1208-1214, 2010.
- [27] J. G. Williams, "The beta relaxation in epoxy resin-based networks," *Journal of applied polymer science*, vol. 23, pp. 3433-3444, 1979.

- [28] D. Colombini, J. Martinez-Vega and G. Merle, "Influence of hydrothermal ageing and thermal treatments on the viscoelastic behavior of DGEBA-MCDEA epoxy resins," *Polym. Bull.*, vol. 48, pp. 75-82, 2002.
- [29] P. Zinck and J.-F. Gérard, "Polyepoxide–water interactions: Influence of the chemical structure of the network," *Polymer Degradation and Stability*, vol. 93, pp. 1231-1237, 2008.
- [30] M. Ochi, M. Yoshizumi and M. Shimbo, "Mechanical and Dielectric Relaxations of Epoxide Resins Containing the Spiro-ring Structure. 11. Effect of the Introduction of Methoxy Branches on Low-temperature Relaxations of Epoxide Resins," *J. Polym. Sci. Part B : Polym Phys*, vol. 25, pp. 1817-1827, 1987.
- [31] F. Kremer and A. Schönhals, *Broadband dielectric spectroscopy*, Springer Science & Business Media, 2012.
- [32] L. Hong, V. Novikov and A. Sokolov, "Is there a connection between fragility of glass forming systems and dynamicheterogeneity/cooperativity?," *J. Non Cryst. Solids*, vol. 357, pp. 351-356, 2011.
- [33] S. Araujo, N. Delpouve, L. Delbreilh, D. Papkov, Y. Dzenis and E. Dargent, "Dielectric and calorimetric signatures of chain orientation in strong and tough ultrafine electrospun polyacrylonitrile," *Polymer*, vol. 178, p. 121638, 2019.
- [34] M. Armand, "Polymers with ionic conductivity," *Advanced Materials*, vol. 2, pp. 278-286, 1990.
- [35] M. A. Ratner, P. Johansson and D. F. Shriver, "Polymer electrolytes: ionic transport mechanisms and relaxation coupling," *Mrs Bulletin*, vol. 25, pp. 31-37, 2000.
- [36] J. D. LeMay and F. N. Kelley, "Structure and ultimate properties of epoxy resins," in *Epoxy Resins and Composites III*, Berlin, 1986.
- [37] J.-P. Pascault and R. J. J. Williams, *Epoxy polymers*, Wiley Online Library, 2010.
- [38] J. D. Keenan, J. C. Seferis and J. T. Quinlivan, "Effects of moisture and stoichiometry on the dynamic mechanical properties of a high-performance structural epoxy," *Journal of applied polymer science*, vol. 24, pp. 2375-2387, 1979.
- [39] M. Ochi, H. Kageyama and M. Shimbo, "Mechanical and dielectric relaxations of poly(hydroxy ethers): 1. Low-temperature relaxations," *Polymer*, vol. 29, pp. 320-324, 1988.
- [40] C. Maggana and P. Pissis, "TSDC studies of the effects of plasticizer and water on the sub-T g relaxations of an epoxy resin system," *Journal of Macromolecular Science, Part B: Physics*, vol. 36, pp. 749-772, 1997.
- [41] S.-W. Kuo, C.-L. Lin and F.-C. Chang, "The study of hydrogen bonding and miscibility in poly(vinylpyridines) with phenolic resin," *Polymer*, vol. 43, pp. 3943-3949, 2002.
- [42] A. K. Jonscher, "Electronic properties of amorphous dielectric films," *Thin Solid Films*, vol. 1, pp. 213-234, 1967.
- [43] M. B. M. Mangion and G. P. Johari, "Relaxations in thermosets. IX. Ionic conductivity and

gelation of DGEBA-based thermosets cured with pure and mixed amines," *Journal of Polymer Science Part B: Polymer Physics*, vol. 29, pp. 1117-1125, 1991.

- [44] R. A. Fava and A. E. Horsfield, "The interpretation of electrical resistivity measurements during epoxy resin cure," *Journal of Physics D: Applied Physics*, vol. 1, p. 117, 1968.

